Am J Transl Res 2024;16(6):2233-2247
www.ajtr.org /ISSN:1943-8141/AJTR0155337

Original Article

Comprehensive analysis of CPNE1 predicts prognosis and drug resistance in gastric adenocarcinoma

Guangyao Li[1], Miaomiao Ping[2], Jizheng Guo[2*], Jin Wang[3*]

[1]Department of Gastrointestinal Surgery, The Second People's Hospital of Wuhu, Wuhu 241000, Anhui, China; [2]School of Basic Medical Sciences, Anhui Medical University, Hefei 230032, Anhui, China; [3]Department of General Surgery, The Traditional Chinese Medicine Hospital of Wuhu, Wuhu 241000, Anhui, China. [*]Equal contributors.

Received January 8, 2024; Accepted May 20, 2024; Epub June 15, 2024; Published June 30, 2024

Abstract: Background: Recent studies have confirmed that Copines-1 (CPNE1) is associated with many malignancies. However, the role of CPNE1 in stomach adenocarcinoma (STAD) is currently unclear. Methods: TIMER2.0, TCGA, UALCAN databases were used to investigate the expression of CPNE1 in STAD and normal tissues. KM-plotter database was used to explore the relationship between CPNE1 expression and prognosis in STAD. Immunohistochemistry (IHC) was used to assess the protein levels of CPNE1 in both normal and cancer tissues, as well as to confirm the prognostic significance of CPNE1. In order to assess the viability of CPNE1 as a divider, the Recipient Operating Characteristics (ROC) curve was employed and the assessment based on the AUC score (below the curve). To investigate the potential function of CPNE1, correlation analysis and enrichment analysis were performed with the clusterProfiler package in R software. The CPNE1 binding protein network was constructed by STRING and GeneMANIA. The relationship between methylation and prognosis was explored by Methsurv database. The Genomics of Drug Sensitivity in Cancer (GDSC) was employed to predict drug responsiveness in STAD. Ultimately, CCK-8 assays and RT-qPCR were performed to confirm the correlation between CPNE1 expression and the IC_{50} of Axitinib in the AGS cell line. Result: CPNE1 is highly expressed in various cancers, including STAD. High expression of CPNE1 indicated poor overall survival (OS) of STAD ($P < 0.05$). The ROC curve suggested that CPNE1 was a potential diagnostic biomarker (AUC = 0.925). The functions of CPNE1 were enriched in DNA-acting catalytic activity, sulfur transferase activity, Ran GTPase binding, DNA helicase activity, helicase activity and eukaryotic ribosome biosynthesis. Hypermethylated CPNE1 predicts better prognosis in STAD ($P < 0.05$). Additionally, STAD patients with high-expression CPNE1 seemed to be more resistant to the chemotherapeutic agents, including A-770041, WH-4-023, AZD-2281, AG-014699, AP-24534, Axitinib, AZD6244, RDEA119, AZD8055, Temsirolimus, Pazopanib and Roscovitine. In vitro experiments demonstrated the involvement of CPNE1 in Axitinib chemoresistance. Conclusion: CPNE1 could be a predictive biomarker and a potential target for biological therapy in STAD.

Keywords: Stomach adenocarcinoma, copines-1, drug resistance, prognosis, immunohistochemical

Introduction

According to the 2020 global cancer statistics, stomach adenocarcinoma (STAD) imposes a significant burden on global healthcare and is prevalent worldwide. It ranks fifth in terms of morbidity and fourth in mortality among all types of carcinoma. In 2020, over one million new cases were diagnosed, and 769,000 people died from stomach cancer [1]. The high aggressiveness of STAD, its heterogeneous nature, low early detection rate, and high relapse rate contribute to a poor prognosis [2]. The mean survival time for STAD patients has been reported as only 12 months, and the 5-year survival rate is as low as 20% in most regions [3]. Despite improvement in the prevention, diagnostic screening, surgical resection, and adjuvant chemotherapy for STAD, further research is still needed to discover and develop more effective clinical treatment.

With the recent advances in high-throughput technologies, targeted therapy has gained interest. Currently, targeted therapies for STAD include anti-HER2 agents (Trastuzumab, Trastuzumab emtansine, Pertuzumab, Lapatinib, Trastuzumab deruxtecan, Margetuximab), anti-

https://doi.org/10.62347/NIYR2094

EGFR agents (Cetuximab and Panitumumab), anti-VEGF agents (Bevacizumab, Ramucirumab, Apatinib, Regorafenib, Sunitinib, Sorafenib), anti-mTOR (Everolimus), anti-HFG/MET agents (Rilotumumab and Onartuzumab), PARP inhibitors (Olaparib), and immunotherapy (Nivolumab, Ipilimumab, Pembrolizumab, Avelumab). However, these treatments do not cover all types of STAD, and their effects are still unsatisfactory [4]. Therefore, there is a need to explore novel prognostic biomarkers and understand their mechanism to improve the diagnosis, treatment choice, and prognosis of STAD.

As an evolutionarily conserved family of phospholipid-binding proteins that depend on calcium, copines share the characteristics of two C2 domains at the N-terminus and one von Willebrand Factor A (VWA) domain at the C-terminus [5]. Currently, nine members have been identified [6]. As the first family member to be discovered, CPNE1 is located at human chromosome 20q11.21 and codes for 537 amino acids. The C2 domain may participate in cellular signal transduction and/or membrane vesicle transport pathways [7]. Previous research has shown that the expression of CPNE1 may play a role in the pathogenesis of carcinogenesis and hepatocellular carcinoma [8], non-small cell lung cancer [9], breast cancer [10], prostate cancer [11], osteosarcoma [12], colorectal cancer [13], and renal cell carcinoma [14]. Song et al. found that silencing of CPNE1 repressed cell proliferation and induced apoptosis by interaction with TRAF2 in pancreatic cancer [15]. Nevertheless, the prognostic significance of CPNE1 in STAD has not been documented, and its underlying mechanism remains unclear.

In this research, the expression of CPNE1 in STAD, its relationship with STAD prognosis, pathogenesis, and drug resistance were explored through the use of bioinformatic analysis. Furthermore, immunohistochemical analysis of clinical specimens was employed to assess the expression of CPNE1 and its prognostic significance in STAD.

Materials and methods

Data acquisition

The STAD gene expression profiles of 375 tumor tissues and 32 normal tissues were obtained from The Cancer Genome Atlas (TCGA) database. Out of the specimens screened above, 32 specimens were paired samples.

Expression of CPNE1

TIMER2.0 database (http://timer.cistrome.org/) was explored to determine pan-cancer CPNE1 expression levels. Different expression of CPNE1 between normal tissue and STAD were analyzed with TCGA data and the UALCAN (http://ualcan.path.uab.edu/analysis.html) online database tool. The feasibility of CPNE1 as a differentiator due to the area under the curve (AUC) score was evaluated using Receiver Operation Properties (ROC) curves.

Survival and prognosis analysis

The KM-plotter database (available at https://kmplot.com/analysis/) was used to evaluate the correlation between CPNE1 expression and prognosis [16]. We used the 206918_s_at probe, which includes survival and CPNE1 expression data from 881 patients. Patients were divided into two groups, high-expression and low-expression, based on the median expression value of CPNE1. Immunohistochemical analyses of the specimens, originating from The Second People's Hospital of Wuhu, were also performed to verify the aforementioned consequences. Before the study commenced, ethical approval was secured from the Ethics Committee of The Second People's Hospital of Wuhu. The study adhered to all relevant regulations.

Co-expression genes and enrichment analysis

To determine the biological function of CPNE1, we selected the top 100 coexpressed genes with a positive correlation with CPNE1 from the GEPIA (http://gepia.cancer-pku.cn/) database. The "enrichGO" function of the R package "clusterProfifiler" was employed to fulfill Gene ontology (GO) enrichment of BP, CC, and MF. The "enrichKEGG" function of the R package clusterProfifiler was used to accomplish Kyoto Encyclopedia of Genomes (KEGG) analysis. In addition, the h.all.v7.2.symbols.gmt [Hallmarks], c2.all.v7.2.symbols.gmt [Curated], and c7.all.v7.2.symbols.gmt [Immunologic signatures] gene sets were chosen for Gene set enrichment analysis (GSEA) with the R package (version 3.6.3). False Discovery Rates (FDR) <

0.25, and p.adjust < 0.05 served as the significant enrichment thresholds.

Analysis of CPNE1 network

The STRING (version 11.5) database (https://string-db.org/), which is a search tool for identifying interactive genes. This had a score (medium confidence) of > 0.4, and size cutoff was selected for no more than 10 interactors. GeneMANIA online database (https://genemania.org/) was used to analyze the intergenic interaction network of CPNE1.

Methylation

MethSurv, an online tool for multivariate survival analysis utilizing DNA methylation data (available at https://biit.cs.ut.ee/methsurv/), was employed to assess the prognostic significance of CpG methylation of CPNE1 in STAD [17].

Immunohistochemistry

Tumor tissues and corresponding non-tumor tissues (located 2 cm away from the tumor edge) were acquired from 110 patients with STAD who underwent curative gastrectomy at The Second People's Hospital of Wuhu, Wuhu, China, between 2011 and 2016, along with clinical information. Immunohistochemical evaluation of CPNE1 was carried out with mouse monoclonal anti-CPNE1 antibody (Abcam, ab155675, 1:500). The specific details for immunohistochemistry were as previously described [18]. The assessment of staining results was performed by two experienced pathologists who were not involved in the experiment. Five random fields of view were selected from each slide at 400× magnification, with a count of 200 cells per field. ImageJ software was used for scoring, where no apparent cell staining was assigned a score of 0; staining in 1% to 10% of cells was scored as 1; staining in 10% to 30% of cells was scored as 2; staining in more than 30% of cells was scored as 3. The staining intensity was also scored as follows: no color or unclear color received a score of 0; pale yellow was scored as 1; light brown was scored as 2; and dark brown was scored as 3. The final score for each slide was the sum of the percentage of staining and the average intensity score. Individuals scoring 3 or above were categorized as exhibiting high expression, whereas individuals scoring less than 3 were categorized as having low expression.

Immunity-related characteristics analysis

The RNAseq data (level 3) and the corresponding clinical information of STAD were obtained from The Cancer Genome Atlas (TCGA) dataset (https://portal.gdc.com). Samples were divided into two groups based on the median value of CPNE1 expression. In order to investigate the relationship between CPNE1 expression and the abundance of tumor-infiltrating immune cells (TIICs), such as B cells, CD4+ T cells, CD8+ T cells, neutrophils, macrophages, and dendritic cells, we conducted immunoscoring using immunedeconv, an R software package that integrates six advanced algorithms, including TIMER, xCell, MCP-counter, CIBERSORT, EPIC, and quanTIseq. Subsequently, immune checkpoint-relevant transcripts including SIGLEC15, TIGIT, CD274, HAVCR2, PDCD1, CTLA4, LAG3, and PDCD1LG2 were chosen, and the expression levels of these eight genes were retrieved. Additionally, we utilized TIMER portals to assess the correlation between CPNE1 expression and immune-related cells. These findings were visualized using the R (v4.0.3) software packages ggplot2 and (or) pheatmap.

The evaluation of drug response

The RNAseq data (level3) and the corresponding clinical information of STD tumors were obtained from the TCGA dataset (https://portal.gdc.com). The largest publicly available pharmacogenomics database [Cancer Drug Sensitivity Genomics (GDSC), https://www.cancerrxgene.org/)] was used to predict differing responses to different chemotherapeutic agents between high and low expression groups. The index of half-maximal inhibitory concentration (IC_{50}) was used for response evaluation. All of the above analytical methods and R software analyses were performed by using the R software, version v4.0.3 (R Foundation for Statistical Computing, 2020).

Cell culture and transient transfection

Four human gastric cancer cell lines (AGS, MGC-803, HGC-27 and GES-1) were procured from Procell Life Science & Technology Co., Ltd. (Wuhan, China). AGS, HGC-27 and GES-1 cells

were cultured in Roswell Park Memorial Institute-1640 (RPMI-1640; Procell), respectively, while MGC-803 cells were grown in high-glucose Dulbecco's modified Eagle's medium (DMEM; Procell). All media were supplemented with 10% fetal bovine serum (FBS; Procell) and 100 mg/mL penicillin-streptomycin solution (Procell), and cells were maintained in a humidified incubator at 37°C with 5% CO_2.

RNA isolation and quantitative real-time PCR

Total RNA was extracted using SparkZol Reagent Kit (AC0101-A, SparkJade). Subsequently, reverse transcription and quantitative real-time PCR (qRT-PCR) were conducted utilizing SPARKscript II RT Kit (AG0304-A, SparkJade). Primer sequences, obtained from TsingkeBiotechnology Co., Ltd. (Beijing, China), were as follows: CPNE1 (forward: 5'-ACCCACTCTGCGTCCTT3', reverse: 5'-TGGCGTCTTGTTGTCTATG-3'). The experimental protocol adhered to procedures previously described by our group [19] and gene expression analysis was conducted using the semiquantitative $2^{-\Delta\Delta Ct}$ method.

Cell proliferation and cytotoxicity assays

Cell viability and proliferation were assessed using the Cell Counting Kit-8 (CCK-8; Biosharp, China) according to manufacturer's instructions. The experimental protocol adhered to a previous study [20].

MTS cell proliferation assay

Axitinib (AG-013736), furnished by Pfizer (La Jolla, CA) in the form of a white powder, was stored at 4°C in a light-free environment. In vitro investigations involved dissolving axitinib in dimethylsulfoxide at a stock concentration of 10 mmol/L, which was then stored at -20°C. Additionally, axitinib was formulated into a homogeneous suspension (5 mg/mL) using 0.5% carboxymethylcellulose (0.5% CMC) and stored at 4°C away from light. AGS cells were plated in 96-well plates at a density of approximately 3,000-5,000 cells per well and incubated overnight in complete medium. Subsequently, the cells were treated with Axitinib. Assessment of cell viability was conducted after 48 hours of drug exposure employing MTS tetrazolium substrate (CellTiter 96 Aqueous One Solution Cell Proliferation Assay; Promega, Madison, WI) following the manufacturer's protocol. The absorbance at 490 nm was measured using a spectrophotometer. Each experiment was replicated three times, with at least triplicates for each concentration.

Statistical methods

The R software (version 4.2.1) and SPSS 17.0 software (SPSS Inc, USA) were employed to carry out all statistical analyses. The differences in CPNE1 expression between unpaired STAD and normal samples from TCGA data were examined by the non-paired Wilcoxon rank sumtest. Furthermore, the paired t-test was employed to assess the differences in 32 paired samples of STAD and adjacent non-cancerous tissues from TCGA data, as well as in CPNE1 immunohistochemical scores between cancerous and adjacent non-cancerous tissues from clinical samples. The area under the curve (AUC) score was evaluated using the Receiver Operating Characteristic (ROC) curves with the pROC package (version 1.17.0.1). Survival analysis was determined by the Survminer package (version 0.4.9). Univariate and multivariate analyses were carried out with survival package (version 3.2-10). *P*-value < 0.05 was considered significant.

Results

CPNE1 pan-cancer expression and expression in STAD

Abnormal expression of CPNE1 was observed in 15 tumors, with elevated expression in 14 tumors, including STAD, and decreased expression in 1 tumor (**Figure 1A**). When compared to the normal samples, increased expression levels of CPNE1 were observed by unpaired (**Figure 1B**, $P < 0.010$) and paired (**Figure 1C**, $P < 0.001$) analyses of gene expression profiles derived from TCGA data in tumor samples. Furthermore, the statistical analysis of the UALCAN database indicated that CPNE1 was overexpressed in STAD compared to the normal samples (**Figure 1D**, $P < 0.01$). The ROC curve demonstrated that the predictive ability of CPNE1 was reasonably accurate for predicting cancer (**Figure 1E**, AUC = 0.925, CI = 0.893-0.957).

Correlation between CPNE1 expression and clinical characteristics in STAD

The level of CPNE1 expression in STAD was explored. The result showed that positive stain-

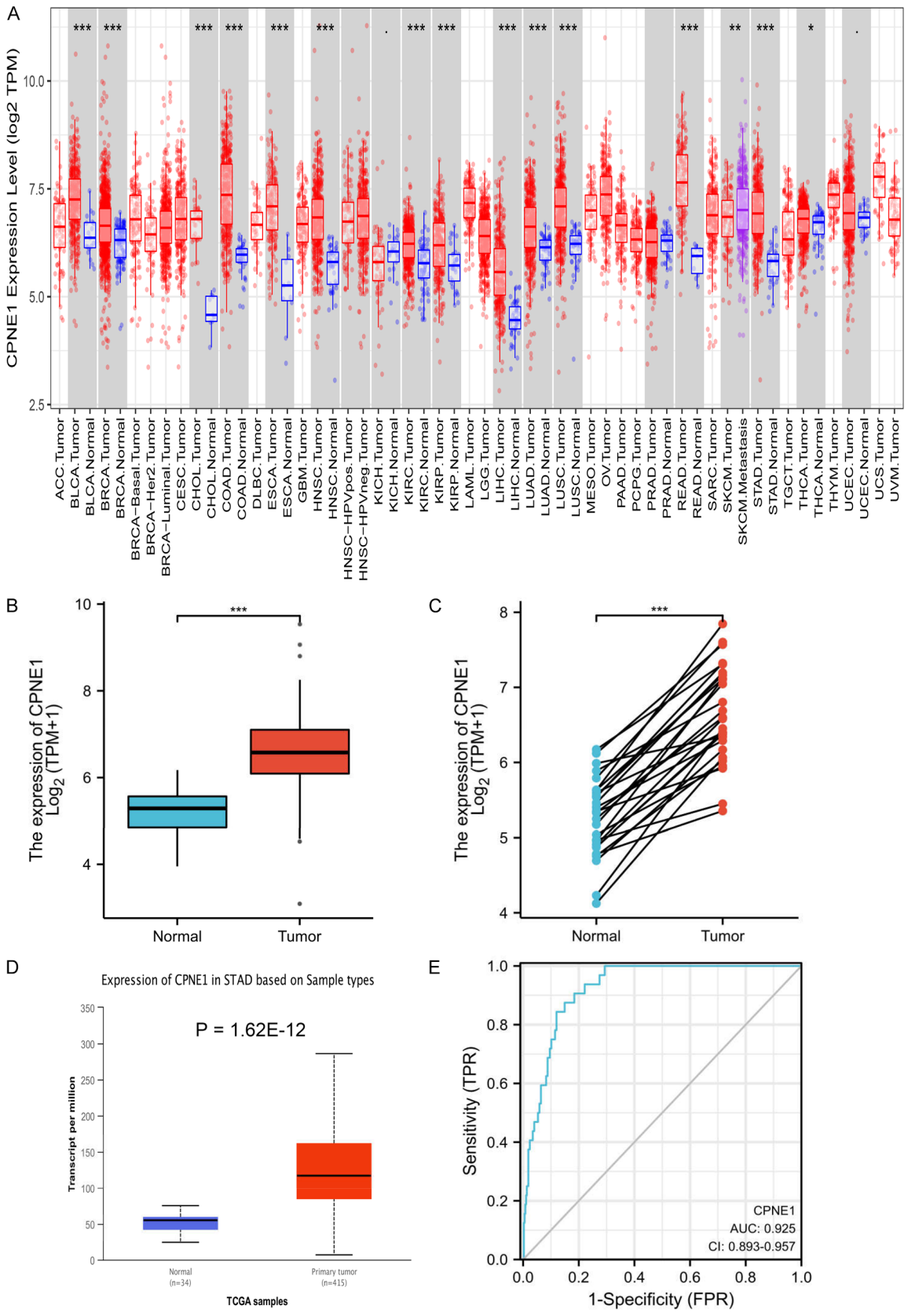
A
CPNE1 Expression Level (log2 TPM)
10.0
7.5
5.0
2.5
ACC.Tumor
BLCA.Tumor
BLCA.Normal
BRCA.Tumor
BRCA.Normal
BRCA−Basal.Tumor
BRCA−Her2.Tumor
BRCA−Luminal.Tumor
CESC.Tumor
CHOL.Tumor
CHOL.Normal
COAD.Tumor
COAD.Normal
DLBC.Tumor
ESCA.Tumor
ESCA.Normal
GBM.Tumor
HNSC.Tumor
HNSC.Normal
HNSC−HPVpos.Tumor
HNSC−HPVneg.Tumor
KICH.Tumor
KICH.Normal
KIRC.Tumor
KIRC.Normal
KIRP.Tumor
KIRP.Normal
LAML.Tumor
LGG.Tumor
LIHC.Tumor
LIHC.Normal
LUAD.Tumor
LUAD.Normal
LUSC.Tumor
LUSC.Normal
MESO.Tumor
OV.Tumor
PAAD.Tumor
PCPG.Tumor
PRAD.Tumor
PRAD.Normal
READ.Tumor
READ.Normal
SARC.Tumor
SKCM.Tumor
SKCM.Metastasis
STAD.Tumor
STAD.Normal
TGCT.Tumor
THCA.Tumor
THCA.Normal
THYM.Tumor
UCEC.Tumor
UCEC.Normal
UCS.Tumor
UVM.Tumor
B
The expression of CPNE1 Log2 (TPM+1)
Normal
Tumor
C
The expression of CPNE1 Log2 (TPM+1)
Normal
Tumor
D
Expression of CPNE1 in STAD based on Sample types
P = 1.62E-12
Transcript per million
Normal (n=34)
Primary tumor (n=415)
TCGA samples
E
Sensitivity (TPR)
1-Specificity (FPR)
CPNE1
AUC: 0.925
CI: 0.893-0.957

Figure 1. Expression of CPNE1 in STAD. (A) Expression levels of CPNE1 in different human cancer tissues compared to normal tissues from the TIMER2.0 database, (B) Expression levels of CPNE1 in unpaired STAD and normal samples from TCGA data, (C) Expression levels of CPNE1 in 32 paired STAD samples and normal from TCGA data, (D) Expression levels of CPNE1 in STAD cancer tissues compared to normal tissue from the UALCAN database, (E) ROC curve indicates that CPNE1 exhibits high accuracy in predicting normal and tumor tissues. *P < 0.05, **P < 0.01, ***P < 0.001.

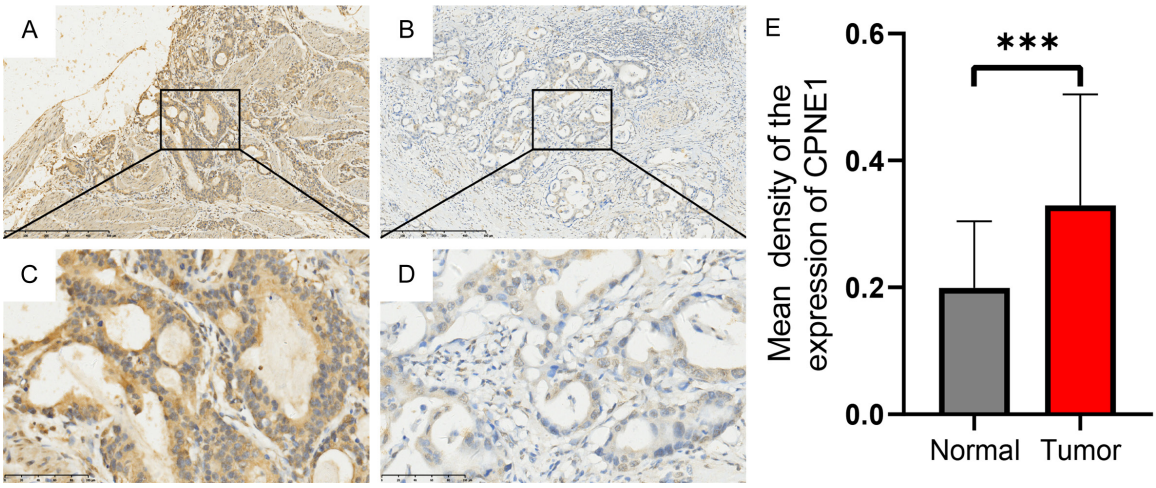

Figure 2. Immunohistochemical detection of CPNE1 expression in STAD tissues. (A) High expression of CPNE1 in STAD tissues (100×), (B) Negative expression of CPNE1 in STAD tissues (100×), (C) High expression of CPNE1 in STAD tissues (400×), (D) Negative expression of CPNE1 in STAD tissues (400×), (E) CPNE1 immunohistochemical scores of normal and tumor tissues. ***P < 0.001.

ing of CPNE1 was predominately present in the cytoplasm of tumor cells and observed in 59.09% (65/110) of STAD tissues (**Figure 2**).

Prognostic value of CPNE1 in STAD

To investigate the connection between CPNE1 expression and the prognosis in STAD, we assessed the prognostic value of CPNE1 using the KM-plotter database. Clearly, higher CPNE1 expression was associated with worse overall survival [HR = 1.73 (1.45-2.08), Logrank P = 1.2e-09] (**Figure 3A**). Additionally, we validated the relationship between CPNE1 expression and prognostic significance in STAD through immunohistochemistry. This demonstrated that CPNE1 overexpression indicated a worse overall survival [HR = 2.11 (1.37-3.23), Logrank P = 0.001] (**Figure 3B**).

Co-expressed genes and enrichment analysis

The top 10 genes associated with CPNE1 were selected from GEPIA, and ggplot2 package [version 3.3.3] was used to show the heatmap. The heatmap indicated that ERGIC3, CTNNBL1, TTI1, ROMO1, SNHG11, SALL4, ASXL1, DHX35, NCOA6, and TPX2 were positively correlated with a high expression of CPNE1 (P < 0.001) (**Figure 4A**). The top 100 genes connected with CPNE1 were collected for GO and KEGG analysis. GO analysis showed that DNA-acting catalytic activity, sulfur transferase activity, Ran GTPase binding, DNA helicase activity and helicase activity were enriched in the molecular function (MF) assay. KEGG data suggested that eukaryotic ribosome biosynthesis was enriched (**Figure 4B**).

GSEA was used to explore the biologic pathways regulated by CPNE1 in STAD between - two groups (high and low) of CPNE1 expression in the TCGA-STAD dataset. The results showed significant enrichment in pathways such as E2F-Targets (NES = 2.018, p.adj = 0.012, FDR = 0.006, **Figure 5A**), G2M-Checkpoint (NES = 1.658, p.adj = 0.012, FDR = 0.006, **Figure 5B**), targets of miR-34B, miR-34C (NES = 1.426, p.adj = 0.028, FDR = 0.019, **Figure 5C**), CD8+ T cells (NES = 1.816, p.adj = 0.030, FDR = 0.017, **Figure 5D**) and B cells (NES = 1.595, p.adj = 0.030, FDR = 0.017, **Figure 5E**).

Co-expression and network analysis

The STRING database was used to perform PPI network analysis and explore potential interac-

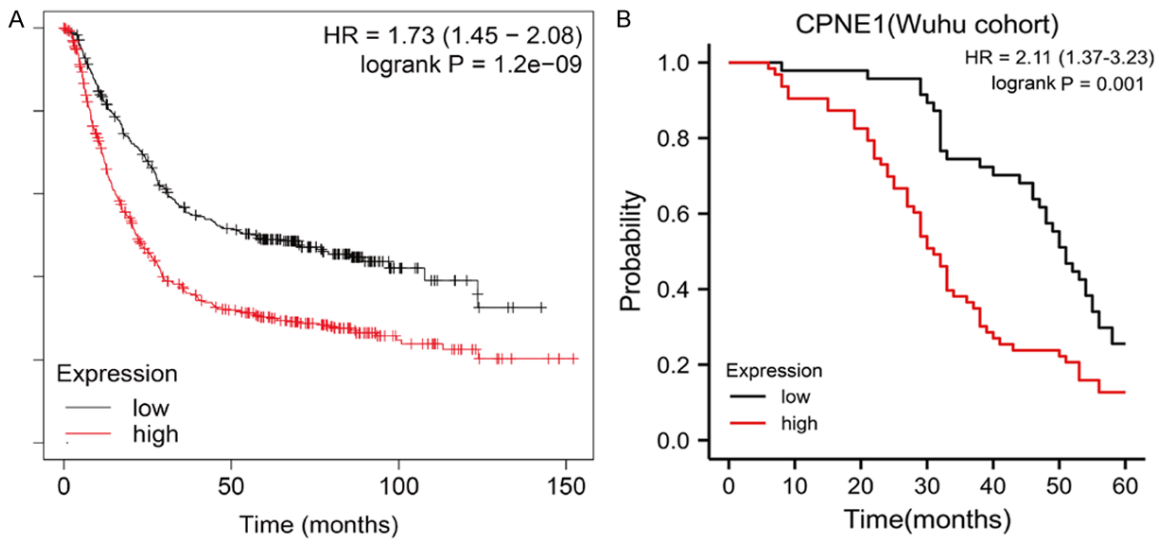

Figure 3. Kaplan-Meier survival curves grouped by high and low CPNE1 expression in STAD patients. (A) Overall survival (OS) in all patients of KMPlotter database, (B) Overall survival (OS) in 110 patients of the Wuhu validated cohort.

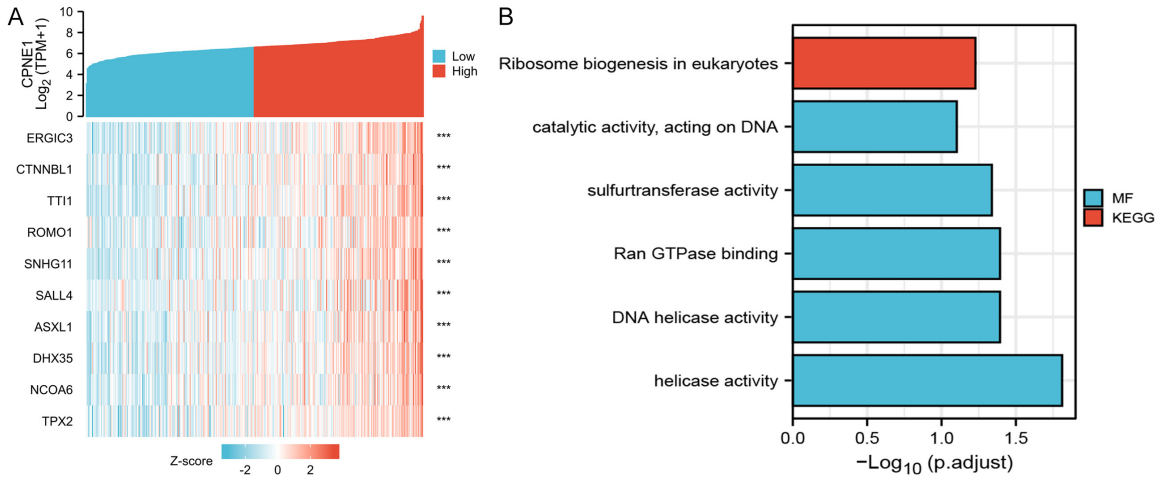

Figure 4. Co-expressed genes and enrichment analysis. (A) Heatmap of the top 10 genes associated with CPNE1 in STAD, (B) Enrichment analysis of the top 100 genes associated with CPNE1 in STAD.

tions among the proteins associated with CPNE1 expression. The ten hub genes were PRKRIP1, LLGL2, FRYL, GGA2, ST3GAL2, PTX4, CRAMP1L, ASCC2, TELO2, and ATP10A (**Figure 6A**). Additionally, GeneMANIA analysis revealed that the top 20 genes were primarily associated with CPNE1 (**Figure 6B**).

Relationship between CpG methylation in CPNE1 and prognosis

A positive correlation between high cg0957-5314 methylation and longer OS was indicated by MethSurv network tool analysis (P = 0.0095) in STAD patients (**Figure 7**). This suggested that hypomethylation of CPNE1, a major epigenetic modification, plays a significant role in carcinogenesis and progression in STAD patients.

CPNE1 may be a biomarker of immune response prediction in STAD

In the above study, we found the CPNE1 expression enriched in abundant immune-associated pathways, prompting us to explore the involvement of CPNE1 in STAD immunotherapy. As shown in **Figure 8A**, CPNE1 expression was associated with the tumor immune cell infiltra-

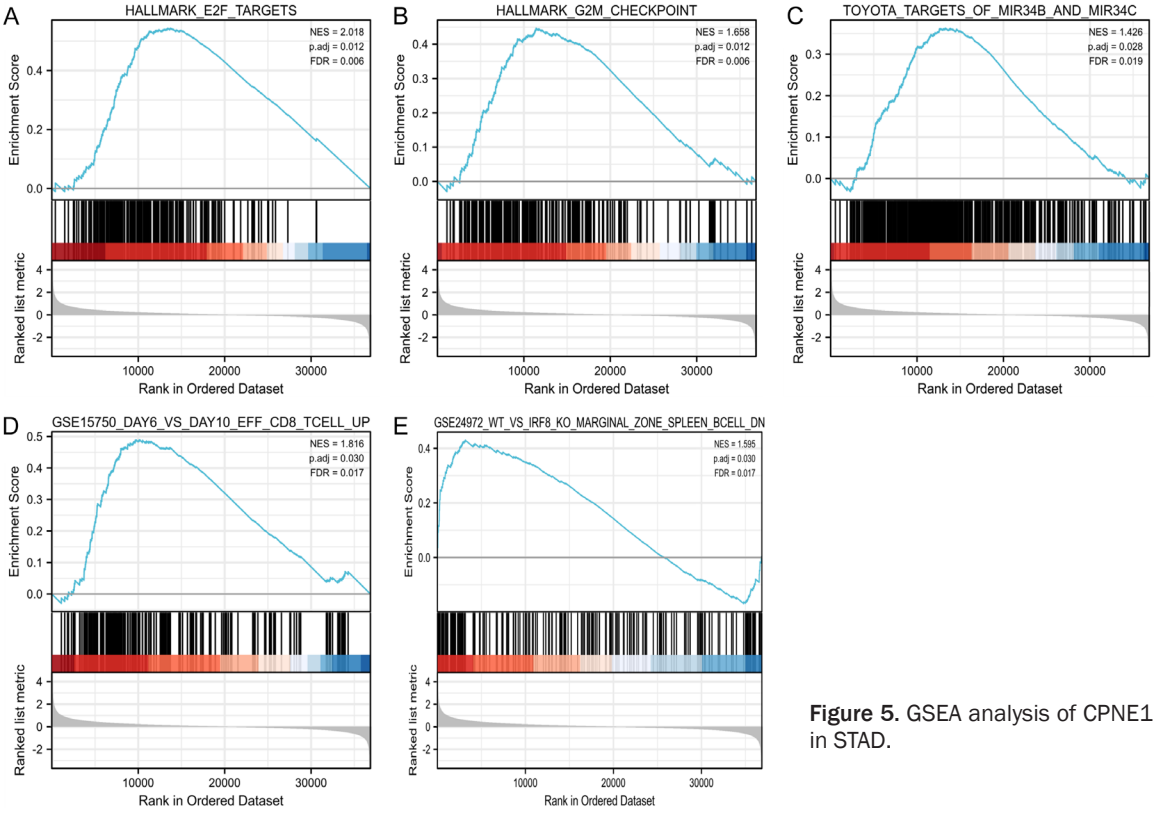

Figure 5. GSEA analysis of CPNE1 in STAD.

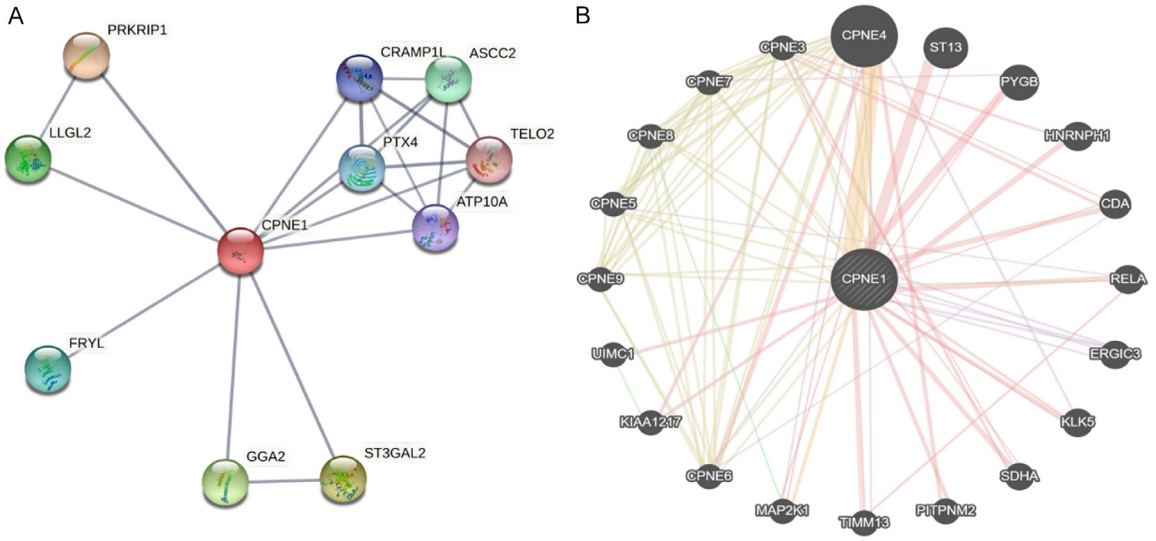

Figure 6. Network analysis of CPNE1 in STRING (A) and GeneMANIA (B) databases. (A) Network analysis of CPNE1 in STRING database, (B) Network analysis of CPNE1 in GeneMANIA database.

tion. Then, we investigated the correlation between CPNE1 expression levels and TIICs to observe if CPNE1 may forecast immunotherapeutic responses in STAD. As shown in **Figure 8C**, CPNE1 expression demonstrated a negative correlation with TIICs in STAD. Furthermore, the association between expression levels of immune checkpoint (ICP) genes and CPNE1 in STAD were explored. The immune checkpoint genes of PDCD1, PDCD1LG2 and SIGLEC15 were upregulated in the low CPNE1 expression group (**Figure 8B**).

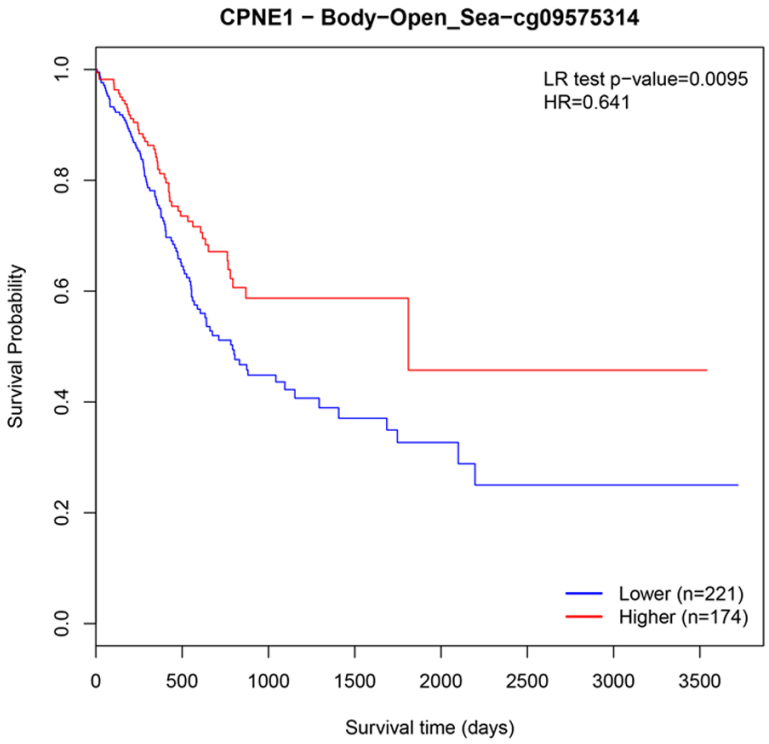

Figure 7. Relationship between CpG methylation in CPNE1 and prognosis. High methylation of cg09575314 in CPNE1 indicates a longer overall survival (OS) in STAD.

Prediction of treatment response to chemotherapy

The cell line data from the GDSC database were employed to predict the IC_{50} of commonly used chemotherapeutic drugs for STAD from TCGA cohort to assess resistance to drugs in high and low expression groups. 11 chemotherapeutic agents (A-770041, WH-4-023, AZD-2281, AG-014699, AP-24534, Axitinib, AZD6244, RDEA119, AZD8055, Temsirolimus, Pazopanib and Roscovitine) exhibited a significantly lower IC_{50} in the low-expression group, indicating that those patients seemed to be more sensitive to the chemotherapeutic agents containing these drugs (**Figure 9A**), while the high-expression group may be more resistant to these drugs. In addition, we plotted the sensitivity of the different expression groups to 10 other commonly used drugs as shown in **Figure 9B**.

Loss-of-function experiments in gastric cancer cells

To explore the function of CPNE1 in cell proliferation and Axitinib resistance, knockdown experiments using siRNA were conducted. Initially, RT-qPCR analyses revealed relatively elevated expression levels of CPNE1 in the three gastric cancer cell lines (AGS, MGC-803, and HGC-27) compared to those in the normal gastric epithelial cell line (GES-1) (**Figure 10A**). Following this, we opted to silence the highest RNA-expressing AGS cell line, which resulted in a silencing efficiency of 77% (**Figure 10B**). The results from the CCK-8 proliferation assay demonstrated a significant decrease in the proliferation rates of the AGS cell line following the knockdown of CPNE1 (**Figure 10C**). Axitinib cytotoxicity assays revealed that the depletion of CPNE1 increased the sensitivity to Axitinib. Notably, this effect varied with concentration. The viability differences were observed at concentration thresholds of 2.14 in the AGS cell line (**Figure 10D**). These results underscore the significance of CPNE1 as a key regulator of cell proliferation and Axitinib sensitivity in gastric cancer.

Discussion

Previous studies have shown that abnormal expression of CPNE1, the first member of the CPNE family to be identified, is closely associated with the biologic behavior of various malignant tumors and hass diverse effects on the proliferation, differentiation, migration, and invasion of tumor cells. Su et al. [8] found that CPNE1 regulates the activation of the AKT/P53 pathway and affects the biologic behavior of hepatocellular carcinoma (LIHC) cells. Additionally, the expression of CPNE1 correlated significantly with tumor immune expansion. Wang et al. [9] proved that CPNE1 interacted with RACK1 through the MET signaling pathway to promote the progression of non-small cell lung cancer. FAK, AKT, ERK, and other signaling pathways could be activated by the overexpression of CPNE1 in tissues and promote the proliferation and metastasis of lung

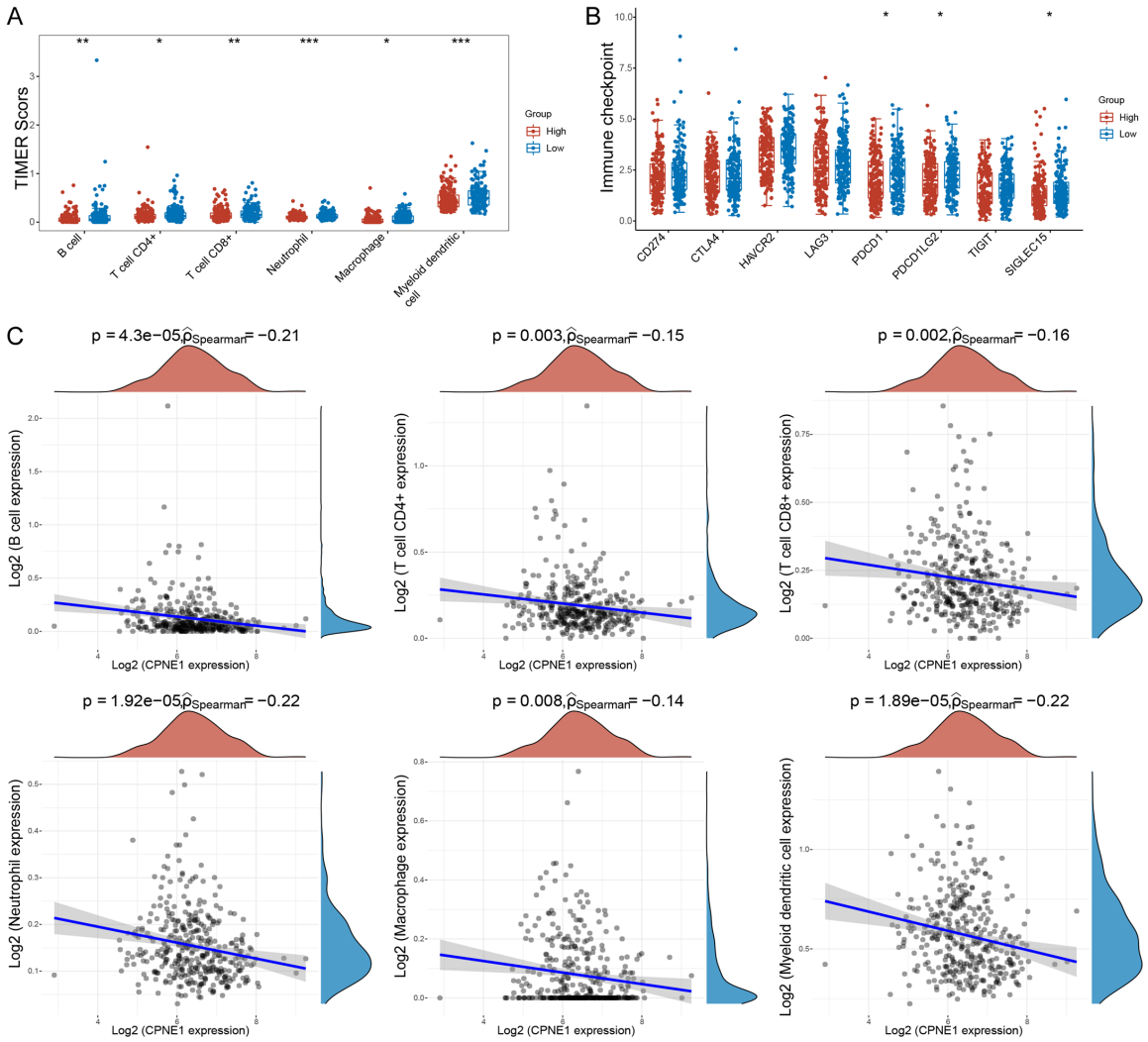

Figure 8. Possible function of CPNE1 in STAD. (A) Correlation of CPNE1 expression with TIMER score of TIICs, including B cells, CD4+, CD8+, Neutrophil, Macrophage and Myeloid dendritic cells, (B) Correlation of CPNE1 expression with immune checkpoint genes, including CD274, CTLA4, HAVCR2, LAG3, PDCD1, PTCD1LG2, TIGIT and SIGLEC15, (C) Correlation result of CPNE1 level and immune infiltration in STAD. *P < 0.05, **P < 0.01, ***P < 0.001.

cancer cells [10, 21]. Wang et al. [13] demonstrated that the AKT/GLUT1/HK2 cascade is activated by CPNE1 which enhanced chemoresistance, and also promoted colorectal cancer progression. However, the prognostic role of CPNE1 in stomach adenocarcinoma (STAD) was not previously reported, and its underlying mechanism was unclear.

Our investigation showed that CPNE1 was overexpressed in STAD relative to normal tissue, which was based on large transcriptome sequencing data from TCGA and immunohistochemistry. The ROC curve also demonstrated the predictive capability of CPNE1 for STAD. We found that the overexpression of CPNE1 was correlated with poor survival. Overall, these results suggested that CPNE1 may be relevant to tumor progression of STAD and serve as a prognostic marker and target for treatment. To investigate the mechanism of CPNE1, GO and KEGG analysis of coexpressed genes and GSEA analysis of CPNE1 were performed. These results of GO and KEGG analyses showed that CPNE1 was mostly associated with Ribosomebiogenesis and had molecular functions including DNA helicase activity, Ran GTPase binding, sulfurtransferase activity and catalytic activity, acting on DNA. Previous studies have shown that quantitative and qualitative changes in ribosomes can lead to deviations in translation patterns and eventually lead to pathogenesis of cancer [22]. The DNA helicases are upregulated in many kinds of can-

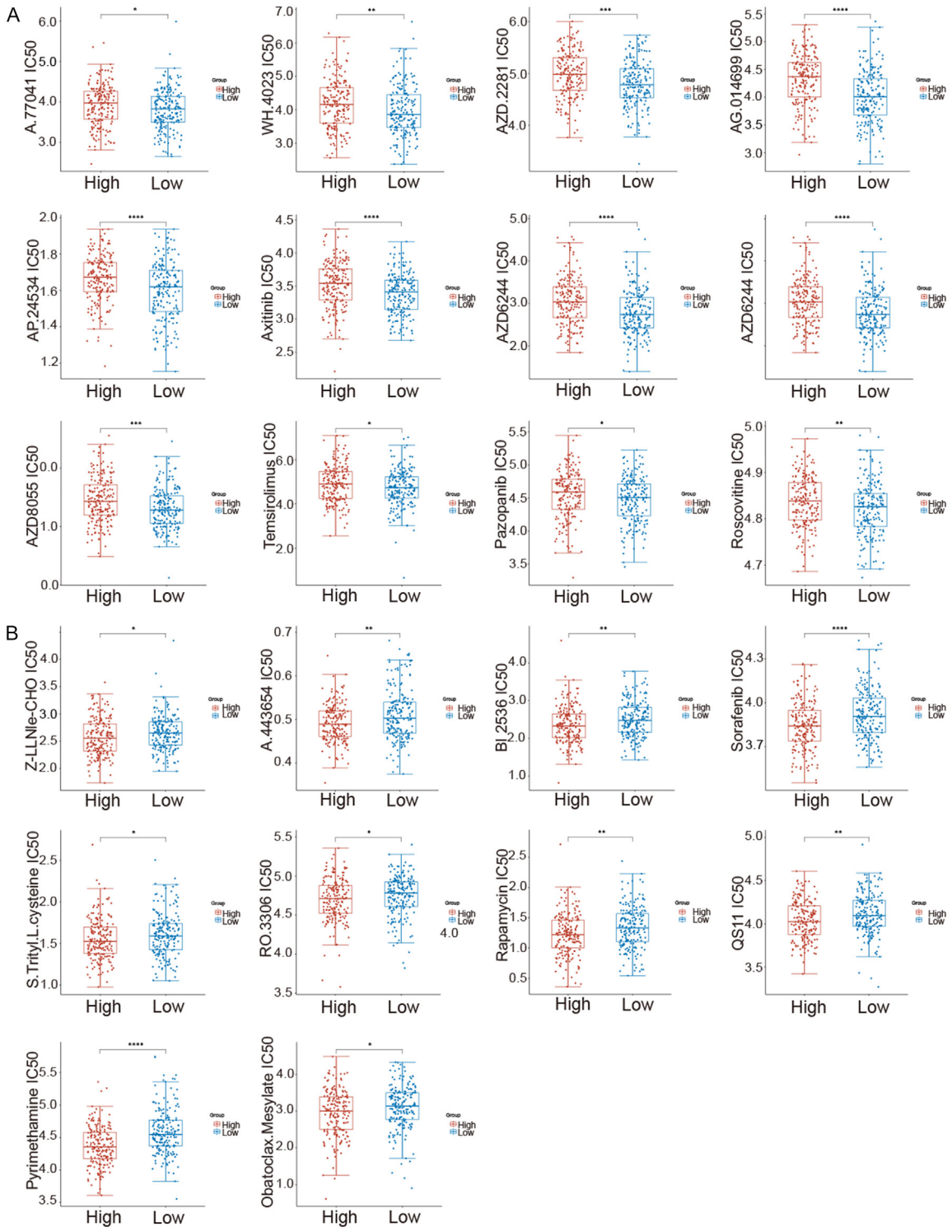

Figure 9. Evaluation of different responses to chemotherapeutic agents between high and low expression groups was conducted by analyzing cell line data from the GDSC database. (A) Resistance of different CPNE 1 expression levels to several commonly used drugs, including A-770041, WH-4-023, AZD-2281, AG-014699, AP-24534, Axitinib, AZD6244, RDEA119, AZD8055, Temsirolimus, Pazopanib and Roscovitine, (B) Sensitivity of the different expression groups to other commonly used chemodrugs, including Z-LLNle-CHO, A-443654, BI-2536, Sorafenib, S-Trityl-L-cysteine, RO-3306, Rapamycin, QS11, Pyrimethamine and Obatoclax Mesylate. *P < 0.05, **P < 0.01, ***P < 0.001.

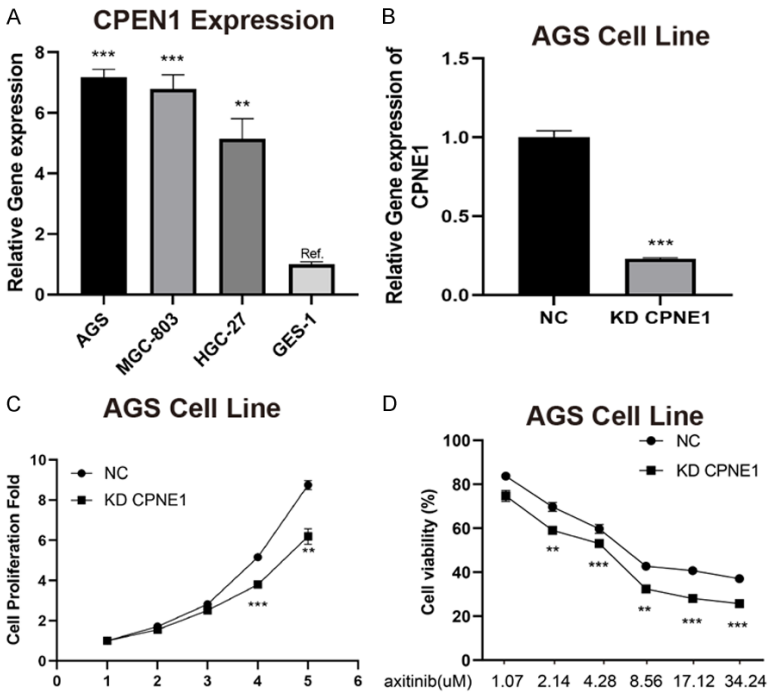

Figure 10. CCK-8 and qRT-PCR assays of gastric cancer cells transfected with CPNE1 siRNA. (A) Relative mRNA expression levels of CPNE1 in three gastric cancer cell lines and GES-1 cells, (B) Knockdown efficacies of CPNE1 siRNA in AGS cell line, (C) Results of CCK-8 proliferation and cytotoxicity experiment in AGS cell line, (D) Inhibition of Axitinib on the AGS cell line. Cells were exposed to various concentrations of Axitinib for 48 h. Cell viability was determined by MtS assay. Axitinib inhibited growth of AGS cell in a dose-dependent manner (n = 3, mean ± SD). *P < 0.05, **P < 0.01, ****P < 0.0001.

cer, and are critical for cancer proliferation. Brosh et al. [23] indicated that several helicase gene mutations were associated with chromosomal instability. GSEA analyses showed that the expression of CPNE1 was enriched in several pathways, such as E2F-Targets, G2M-Checkpoint, targets of mir-34B and mir-34C, CD8+ T cells and B cells. The E2F family primarily regulates cell cycle progression and DNA synthesis and has been demonstrated to be linked with different types of tumors, including STAD [24]. The G2M checkpoint is the final checkpoint that regulates the cell cycle and prevents DNA damaged cells from entering mitosis [25]. Abnormalities of this checkpoint will lead to an abnormal cell cycle and ultimately lead to tumorigenesis and progression [26]. These suggest that CPNE1 may be involved in the cell cycle and participate in the occurrence and progression of STAD. In the current study, we also found the CPNE1 expression was enriched in CD8+ T cells-UP and B cells-DN pathways.

To comprehensively analyze the function of CPNE1 in STAD, we analyzed the genes (ERGIC3, CTNNBL1, TTI1, ROMO1, SNHG11, SALL4, ASXL1, DHX35, NCOA6 and TPX2) that were significantly related to CPNE1 expression in STAD. Zhao et al. [27] also observed that the combined silencing of ERGIC3 and BFA treatment could synergistically impede the growth of lung cancer cells. The research of Li et al. [28] showed that CTNNBL1 promotes proliferation and invasion in ovarian cancer. Our results confirmed that it may promote gastric cancer cell proliferation and invasion. The PPI network and GeneMANIA also showed the protein interaction between CPNE1 and other partners may play roles in the progression and invasion of tumors.

As one of the most important epigenetic processes that govern gene expression, DNA methylation is extremely dynamic during development and specific to somatic cells. Deviations from normal DNA methylation patterns are strongly associated with human diseases, including malignant tumors [29]. In this study, we found that DNA hypomethylation, an important epigenetic modification, can induce CPNE1 expression at the transcriptional level. Therefore, it also plays a significant role in carcinogenesis and progression of STAD.

We analyzed the immune microenvironment and observed that CPNE1 expression was associated with TIICs and immune checkpoints. The infiltration of immune cells and their interactions with cancer cells have shaped a distinct tumor immune microenvironment (TIME). It has been established that TIICs play a broad role in various aspects of cancer progression [30], which include immune evasion, metastasis, drug responses, and the prognosis of cancer patients. In this study, we observed that the low expression of CPNE1 was associated with

higher TIMER scores of TIICs and demonstrated a negative correlation between CPNE1 expression and TIICs in STAD. These results demonstrated that CPNE1 may play a regulatory role of the immune microenvironment. Additionally, we observed an association between decreased CPNE1 expression and heightened levels of the immune checkpoint proteins (ICPs) PDCD1, PDCD1LG2, and SIGLEC15. This implies that CPNE1 expression influences the immune microenvironment in STAD tissues by impacting the expression of ICPs. Therefore, CPNE1 holds promise as an immunotherapy biomarker and prognosticator for tumor immunotherapeutic response.

Drug resistance represents an important challenge to improving the outcome for STAD patients. Our study has shown that high-expression CPNE1 appeared to be more resistant to chemotherapeutic agents, including A-770041, WH-4-023, AZD-2281, AG-014699, AP-24534, Axitinib, AZD6244, RDEA119, AZD8055, Temsirolimus, Pazopanib, and Roscovitine. A-770041 and WH-4-023 are potent LCK inhibitors of Src family. They inhibit cell growth, prevent cell migration, and induce cell autophagy by halting cell cycle progression at the G1/S phase. PARP inhibitors, such as AZD-2281 and AG014699, can treat cancers with DNA repair defects, such as those harboring a BRCA1 or BRCA2 (BRCA1/2) mutation, by rendering them deficient in homologous recombination repair [31]. AP24534 and Axitinib are multitarget kinase inhibitors, both of them exert their antiangiogenic effects by blocking signaling mediated by VEGFRs, PDGFRs, and c-Kit. Our investigation demonstrated that axitinib alone exhibited a dose-dependent inhibition of AGS gastric cancer cell growth in vitro. AZD6244 and RDEA119 are MEK inhibitors. AZD6244, in combination with chemotherapy, has shown beneficial effects in STAD [32]. AZD8055 and Temsirolimus are mTOR kinase inhibitors that can block cancer cell proliferation and/or induce cancer cell death, which may be contribute to treatment of STAD patients [33, 34]. Palbociclib and Roscovitine are CDK inhibitors, these can inhibit the cell cycle and anti-tumor cell proliferative activity and may have therapeutic benefits for STAD [35, 36]. In addition, our study found that high-expression CPNE1 seemed to be more sensitive to S-Trityl-L-cysteine, RO-3306, Rapamycin, QS11, Pyrimethamine and Obatoclax-Mesylate, which may be therapeutic options for the high-expression group. Our study sheds light on the role of CPNE1 in STAD progression and its association with some drug resistance, including Axitinib. Understanding the mechanisms underlying tumor development and drug resistance is crucial for identifying therapeutic targets for personalized treatment. The identification of CPNE1 as a key player in STAD provides a promising opportunity for the development of novel therapeutic interventions. In summary, our findings highlight the significance of CPNE1 in STAD and provide a foundation for future translational research.

Although we used bioinformatic methodsto explored the association between CPNE1 expression and the prognosis of gastric cancer, we preliminarily investigated potential underlying mechanisms. Weinvestigated the association between CPNE1 methylation and gastric cancer prognosis, explored the association between CPNE1 expression and immune infiltration, as well as immune checkpoint expression, explored the association between CPNE1 expression and resistance to potential therapeutic drugs, and validated the relationship between CPNE1 expression and STAD prognosis using immunohistochemistry, we have not carried out sufficient in vivo and in vitro experiments to verify its mechanisms. The underlying mechanism needs to be further validated. In the future, we plan to conduct both in vitro and in vivo experiments to investigate the specific mechanisms by which CPNE1 participates in the development of STAD and its involvement in drug resistance.

Conclusion

Our study demonstrated that CPNE1 expression is upregulated in STAD and strongly associated with poor survival. Additionally, CPNE1 expression is linked to ribosome biogenesis, DNA helicase activity, cell cycle, tumor infiltrating immune, and DNA methylation. Furthermore,, CPNE1 expression correlates with resistance to certain drugs, notably axitinib. These findings collectively suggest that CPNE1 may serve as a predictive biomarker and target for therapy in STAD.

Acknowledgements

The authors would like to express their sincere gratitude to the TCGA databases for providing

the data, as well as to TIMER2.0, KM plotter, UALCAN, GEPIA, STRING, GeneMANIA, Methsurv databases, and GDSC for providing online analysis tools. This study was funded by Wannan Medical University Natural Science Foundation (Grant No. JXYY202297) and Anhui Provincial Health Commission Provincial Support for Youth Programs (Grant No. AHWJ2023A30159).

Informed consent was obtained from all patients participating this study.

Disclosure of conflict of interest

None.

Address correspondence to: Jizheng Guo, School of Basic Medical Sciences, Anhui Medical University, Hefei 230032, Anhui, China. E-mail: guojizheng@ahmu.edu.cn; Jin Wang, Department of General Surgery, The Traditional Chinese Medicine Hospital of Wuhu, Wuhu 241000, Anhui, China. E-mail: 2016150302@jou.edu.cn

References

[1] Sung H, Ferlay J, Siegel RL, Laversanne M, Soerjomataram I, Jemal A and Bray F. Global cancer statistics 2020: GLOBOCAN estimates of incidence and mortality worldwide for 36 cancers in 185 countries. CA Cancer J Clin 2021; 71: 209-249.

[2] Zhou L, Li SH, Wu Y and Xin L. Establishment of a prognostic model of four genes in gastric cancer based on multiple data sets. Cancer Med 2021; 10: 3309-3322.

[3] Yoon SJ, Kim JY, Long NP, Min JE, Kim HM, Yoon JH, Anh NH, Park MC, Kwon SW and Lee SK. Comprehensive multi-omics analysis reveals aberrant metabolism of epstein-barr-virus-associated gastric carcinoma. Cells 2019; 8: 1220.

[4] Patel TH and Cecchini M. Targeted therapies in advanced gastric cancer. Curr Treat Options Oncol 2020; 21: 70.

[5] Creutz CE, Tomsig JL, Snyder SL, Gautier MC, Skouri F, Beisson J and Cohen J. The copines, a novel class of C2 domain-containing, calcium-dependent, phospholipid-binding proteins conserved from Paramecium to humans. J Biol Chem 1998; 273: 1393-402.

[6] Tomsig JL and Creutz CE. Copines: a ubiquitous family of Ca(2+)-dependent phospholipid-binding proteins. Cell Mol Life Sci 2020; 59: 1467-77.

[7] Yang W, Ng P, Zhao M, Wong TK, Yiu SM and Lau YL. Promoter-sharing by different genes in human genome--CPNE1 and RBM12 gene pair as an example. BMC Genomics 2008; 9: 456.

[8] Su J, Huang Y, Wang Y, Li R, Deng W, Zhang H and Xiong H. CPNE1 is a potential prognostic biomarker, associated with immune infiltrates and promotes progression of hepatocellular carcinoma. Cancer Cell Int 2022; 22: 67.

[9] Wang A, Yang W, Li Y, Zhang Y, Zhou J, Zhang R, Zhang W, Zhu J, Zeng Y, Liu Z and Huang JA. CPNE1 promotes non-small cell lung cancer progression by interacting with RACK1 via the MET signaling pathway. Cell Commun Signal 2022; 20: 16.

[10] Shao Z, Ma X, Zhang Y, Sun Y, Lv W, He K, Xia R, Wang P and Gao X. CPNE1 predicts poor prognosis and promotes tumorigenesis and radioresistance via the AKT singling pathway in triple-negative breast cancer. Mol Carcinog 2020; 59: 533-544.

[11] Liang J, Zhang J, Ruan J, Mi Y, Hu Q, Wang Z and Wei B. CPNE1 is a useful prognostic marker and is associated with TNF Receptor-Associated Factor 2 (TRAF2) expression in prostate cancer. Med Sci Monit 2017; 23: 5504-5514.

[12] Jiang Z, Jiang J, Zhao B, Yang H, Wang Y, Guo S, Deng Y, Lu D, Ma T, Wang H and Wang J. CPNE1 silencing inhibits the proliferation, invasion and migration of human osteosarcoma cells. Oncol Rep 2018; 39: 643-650.

[13] Wang Y, Pan S, He X, Wang Y, Huang H, Chen J, Zhang Y, Zhang Z and Qin X. CPNE1 enhances colorectal cancer cell growth, glycolysis, and drug resistance through regulating the AKT-GLUT1/HK2 pathway. Onco Targets Ther 2021; 14: 699-710.

[14] Talaat IM, Abu-Gharbieh E, Hussein A, Hachim M, Sobhy I, Eladl M and El-Huneidi W. Prognostic value of copine 1 in patients with renal cell carcinoma. Anticancer Res 2022; 42: 355-362.

[15] Song Y, Song B, Yu Z, Li A, Xia L, Zhao Y, Lu Z and Li Z. Silencing of CPNE1-TRAF2 axis restrains the development of pancreatic cancer. Front Biosci (Landmark Ed) 2023; 28: 316.

[16] Lánczky A and Győrffy B. Web-based survival analysis tool tailored for medical research (KMplot): development and implementation. J Med Internet Res 2021; 23: e27633.

[17] Modhukur V, Iljasenko T, Metsalu T, Lokk K, Laisk-Podar T and Vilo J. MethSurv: a web tool to perform multivariable survival analysis using DNA methylation data. Epigenomics 2018; 10: 277-288.

[18] Li GY, Huang M, Pan TT and Jia WD. Expression and prognostic significance of contactin 1 in human hepatocellular carcinoma. Onco Targets Ther 2016; 9: 387-94.

[19] Li G, Ping M, Zhang W, Wang Y, Zhang Z and Su Z. Establishment of the molecular subtypes

and a risk model for stomach adenocarcinoma based on genes related to reactive oxygen species. Heliyon 2024; 10: e27079.
[20] Chen J, Liu Z, Wu Z, Li W and Tan X. Identification of a chemoresistance-related prognostic gene signature by comprehensive analysis and experimental validation in pancreatic cancer. Front Oncol 2023; 13: 1132424.
[21] Liu S, Tang H, Zhu J, Ding H, Zeng Y, Du W, Ding Z, Song P, Zhang Y, Liu Z and Huang JA. High expression of Copine 1 promotes cell growth and metastasis in human lung adenocarcinoma. Int J Oncol 2018; 53: 2369-2378.
[22] Wang X, Zhang H, Sapio R, Yang J, Wong J, Zhang X, Guo JY, Pine S, Van Remmen H, Li H, White E, Liu C, Kiledjian M, Pestov DG and Steven Zheng XF. SOD1 regulates ribosome biogenesis in KRAS mutant non-small cell lung cancer. Nat Commun 2021; 12: 2259.
[23] Datta A and Brosh RM Jr. New insights into DNA helicases as druggable targets for cancer therapy. Front Mol Biosci 2018; 5: 59.
[24] Kent LN and Leone G. The broken cycle: E2F dysfunction in cancer. Nat Rev Cancer 2019; 19: 326-338.
[25] Asghar U, Witkiewicz AK, Turner NC and Knudsen ES. The history and future of targeting cyclin-dependent kinases in cancer therapy. Nat Rev Drug Discov 2015; 14: 130-46.
[26] Guo H, Zeng B, Wang L, Ge C, Zuo X, Li Y, Ding W, Deng L, Zhang J, Qian X, Song X and Zhang P. Knockdown CYP2S1 inhibits lung cancer cells proliferation and migration. Cancer Biomark 2021; 32: 531-539.
[27] Zhao Q, Wu M, Zheng X, Yang L, Zhang Z, Li X and Chen J. ERGIC3 silencing additively enhances the growth inhibition of BFA on lung adenocarcinoma cells. Curr Cancer Drug Targets 2020; 20: 67-75.
[28] Li Y, Guo H, Jin C, Qiu C, Gao M, Zhang L, Liu Z and Kong B. Spliceosome-associated factor CTNNBL1 promotes proliferation and invasion in ovarian cancer. Exp Cell Res 2017; 357: 124-134.
[29] Huang W, Li H, Yu Q, Xiao W and Wang DO. LncRNA-mediated DNA methylation: an emerging mechanism in cancer and beyond. J Exp Clin Cancer Res 2022; 41: 100.
[30] Bai Y, Li C, Xia L, Gan F, Zeng Z, Zhang C, Deng Y, Xu Y, Liu C, Deng S and Liu L. Identifies immune feature genes for prediction of chemotherapy benefit in cancer. J Cancer 2022; 13: 496-507.
[31] Nakamura K, Takae S, Shiraishi E, Shinya K, Igualada AJ and Suzuki N. Poly (ADP-ribose) polymerase inhibitor exposure reduces ovarian reserve followed by dysfunction in granulosa cells. Sci Rep 2020; 10: 17058.
[32] Ahn S, Brant R, Sharpe A, Dry JR, Hodgson DR, Kilgour E, Kim K, Kim ST, Park SH, Kang WK, Kim KM and Lee J. Correlation between MEK signature and Ras gene alteration in advanced gastric cancer. Oncotarget 2017; 8: 107492-107499.
[33] Liu W, Chang J, Liu M, Yuan J, Zhang J, Qin J, Xia X and Wang Y. Quantitative proteomics profiling reveals activation of mTOR pathway in trastuzumab resistance. Oncotarget 2017; 8: 45793-45806.
[34] Guo G, Zhou Z, Chen S, Cheng J, Wang Y, Lan T and Ye Y. Characterization of the prognosis and tumor microenvironment of cellular senescence-related genes through scRNA-Seq and bulk RNA-Seq analysis in GC. Recent Pat Anticancer Drug Discov 2023; [Epub ahead of print].
[35] Bi H, Shang J, Zou X, Xu J and Han Y. Palbociclib induces cell senescence and apoptosis of gastric cancer cells by inhibiting the Notch pathway. Oncol Lett 2021; 22: 603.
[36] Iseki H, Ko TC, Xue XY, Seapan A, Hellmich MR and Townsend CM Jr. Cyclin-dependent kinase inhibitors block proliferation of human gastric cancer cells. Surgery 1997; 122: 187-194.